Supporting Information

A novel displacement-type colorimetric chemosensor for the detection of Cu^{2+} and GSH in aqueous solution

Ga Rim You, Hyo Jung Jang, Tae Geun Jo, Cheal Kim*

Department of Fine Chemistry and Department of Interdisciplinary Bio IT Materials, Seoul National University of Science and Technology, Seoul 139-743, Korea. Fax: +82-2-973-9149; Tel: +82-2-970-6693; E-mail: chealkim@seoultech.ac.kr

Table S1. Examples for the detection of Cu^{2+} by colorimetric chemosensors

Colorimetric chemosensor	Analyte	Sequence	Binding constant (M^{-1})	Detection limit (μM)	Reference
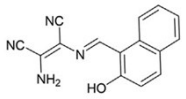	Cu	Cys	3.2×10^{4}	2.4	[1]
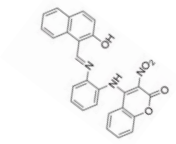	Cu	CN	5.0×10^{3}	29.5	[2]
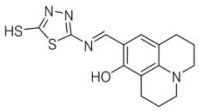	Cu	CN	1.0×10^{10}	0.9	[3]
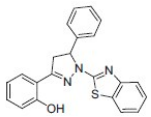	Cu	None	9.3×10^{4}	0.087	[4]
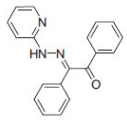	Cu	None	5.7×10^{8}	0.0825	[5]
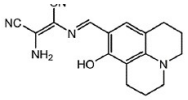	Cu	None	2.3×10^{4}	2.4	[6]
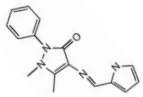	Cu	None	8.3×10^{4}	0.217	[7]
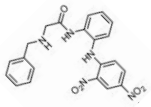	Cu	None	1.3×10^{3}	0.26	[8]
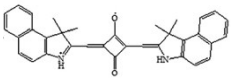	Cu	None	4.1×10^{4}	59	[9]
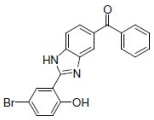	Cu	None	3.3×10^{6}	1	[10]
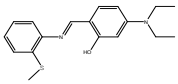	Cu	GSH	1.0×10^{4}	3.89	This work

References

1 S. A. Lee, J. J. Lee, J. W. Shin, K. S. Min and C. Kim, *Dye. Pigment.*, 2015, **116**, 131-138.

2 H. Y. Jo, G. J. Park, Y. J. Na, Y. W. Choi, G. R. You and C. Kim, *Dye. Pigment.*, 2014, **109**, 127-134.

3 G. R. You, G. J. Park, J. J. Lee and C. Kim, *Dalton Trans.*, 2015, **44**, 9120-9129.

4 S. Hu, S. Zhang, Y. Hu, Q. Tao and A. Wu, *Dye. Pigment.*, 2013, **96**, 509-515.

5 S. Hu, J. Song, F. Zhao, X. Meng and G. Wu, *Sensors Actuators B Chem.*, 2015, **215**, 241-248.

6 T. G. Jo, Y. J. Na, J. J. Lee, M. M. Lee, S. Y. Lee and C. Kim, *Sensors Actuators, B Chem.*, 2015, **211**, 498-506.

7 J.-J. Xiong, P.-C. Huang, C.-Y. Zhang and F.-Y. Wu, *Sensors Actuators B Chem.*, 2016, **226**, 30-36.

8 S.-L. Kao, W.-Y. Lin, P. Venkatesan and S.-P. Wu, *Sensors Actuators B Chem.*, 2014, **204**, 688-693.

9 Y. Wang, C. Wang, S. Xue, Q. Liang, Z. Li and S. Xu, *RSC Adv.*, 2016, **6**, 6540-6550.

10 A. Sen Gupta, K. Paul and V. Luxami, *Inorg. Chim. Acta*, 2016, **443**, 57-63

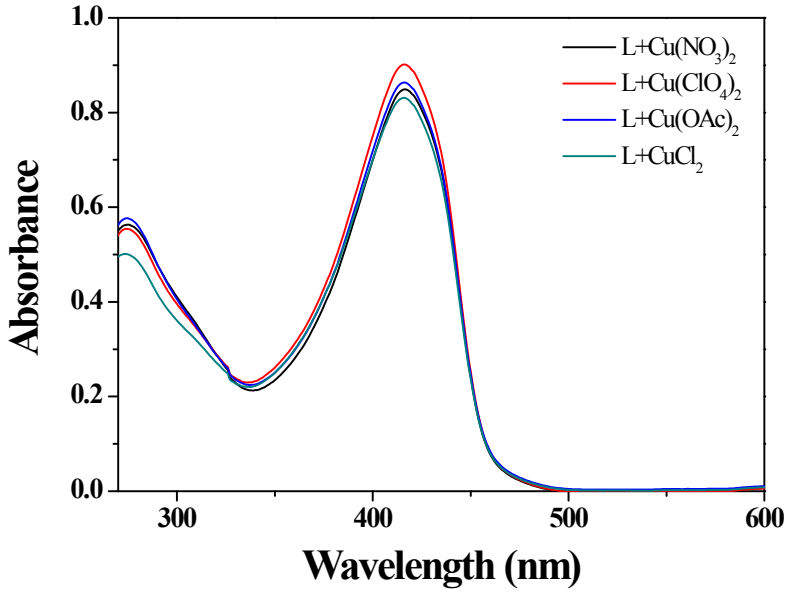

Fig. S1 Absorption spectra of **1** (30 μM) upon the addition of 5 equiv of various copper salts in DMF/bis-tris buffer (7/3; v/v. 10 mM bis-tris, pH = 7.0).

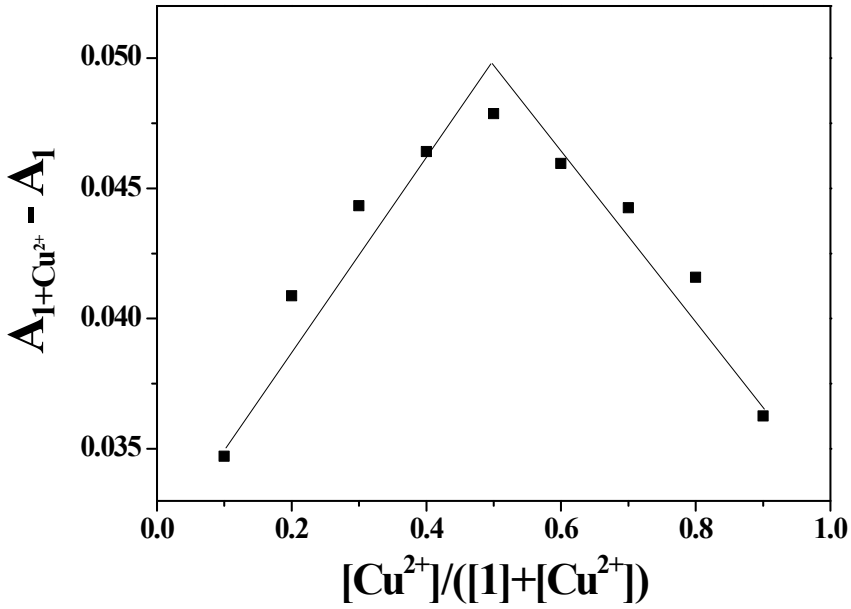

Fig S2. Job plot of **1** and Cu^{2+}, where the intensity at 416 nm was plotted against the mole fraction of Cu^{2+}. The total concentration of Cu^{2+} with receptor **1** was 3.0×10^{-5} M.

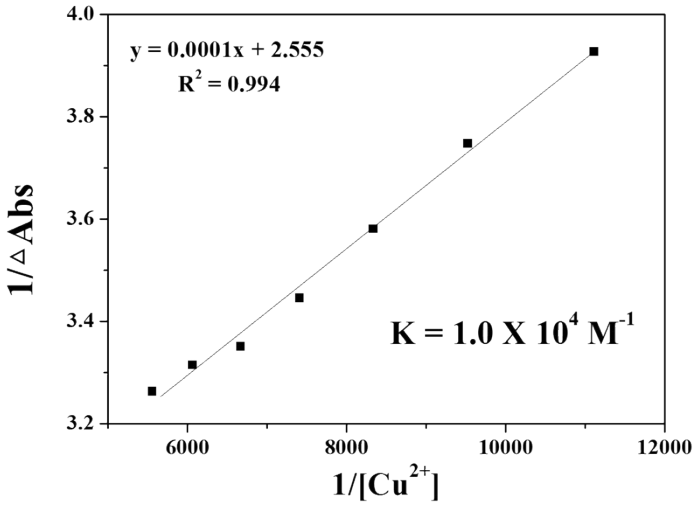

Fig. S3 Benesi-Hildebrand plot (at 416 nm) of **1** (30 μM), assuming 1:1 stoichiometry for association between **1** and Cu^{2+}.

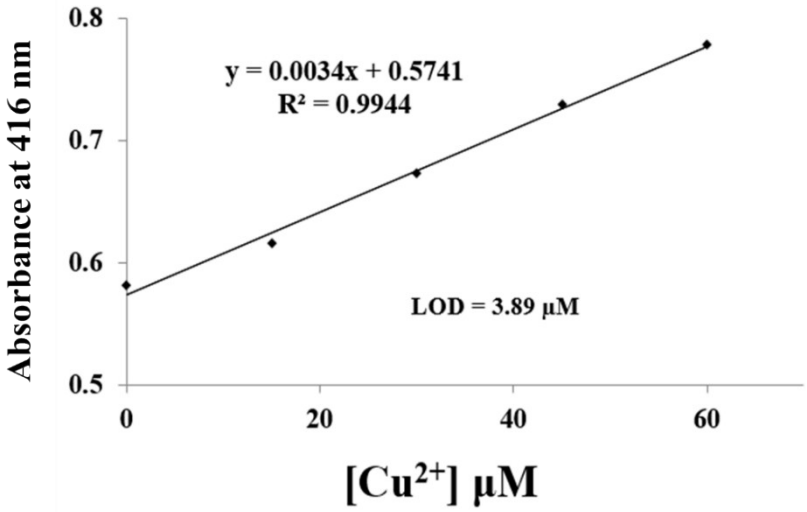

Fig. S4 Determination of the detection limit of **1** (30 μM) for Cu^{+} based on change of absorbance at 416 nm.

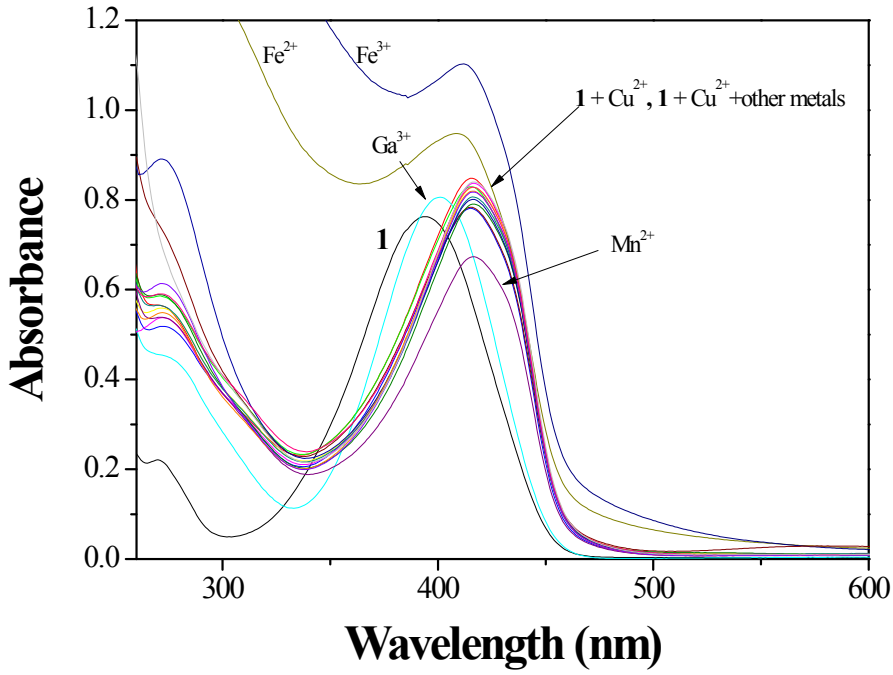

(a)

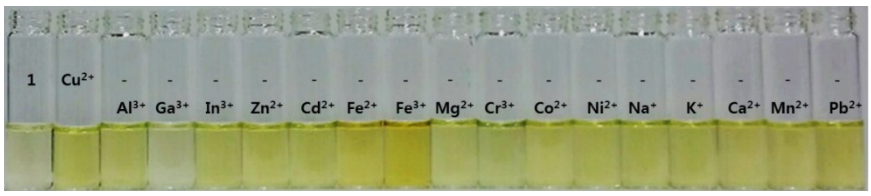

(b)

Fig. S5 (a) Absorption spectral changes of competitive selectivity of **1** (30 μM) toward Cu^{2+} (5 equiv) in the presence of other metal ions (25 equiv) in DMF/bis-tris buffer (7/3, v/v). (b) The color changes of competitive selectivity of **1** (30 μM) toward Cu^{2+} (5 equiv) in the presence of other metal ions (25 equiv).

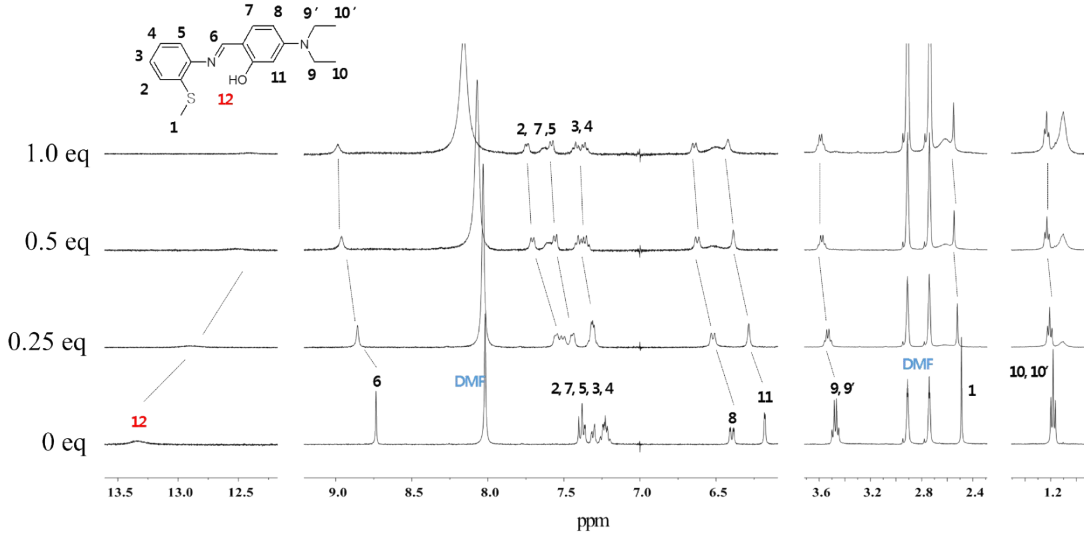

Fig. S6 ^{1}H NMR titration of **1** with Cu^{2+}.

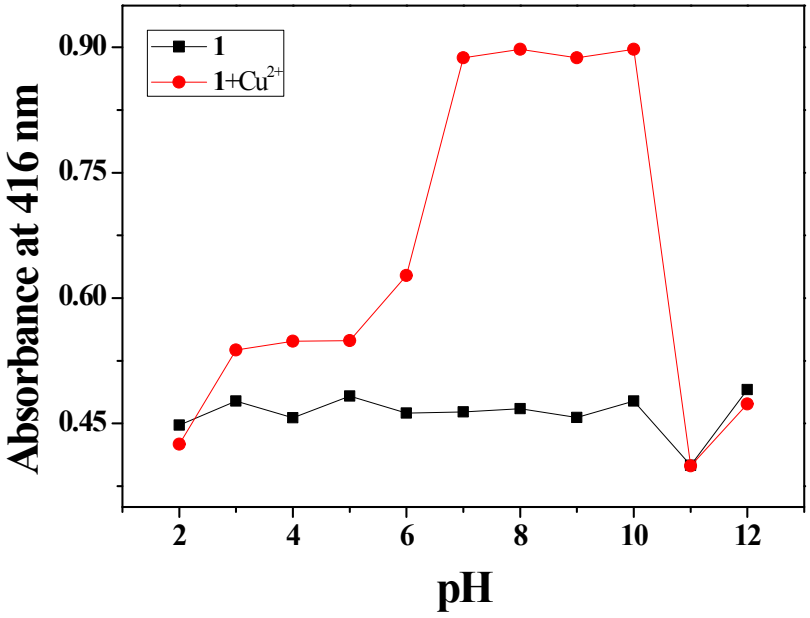

Fig. S7 UV absorbance (at 416 nm) of **1** (30 μM) and **1**-Cu^{2+} complex at different pH (2-12) in a mixture of DMF/bis-tris buffer (7/3, v/v), respectively.

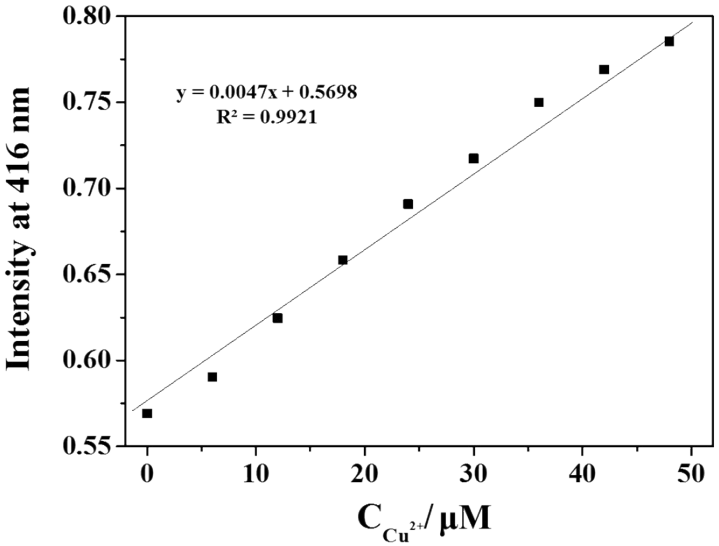

Fig. S8 Absorption (at 416 nm) of **1** as a function of Cu^{2+} concentration. [**1**] = 30 μmol/L and [Cu^{2+}] = 0-48.0 μmol/L.

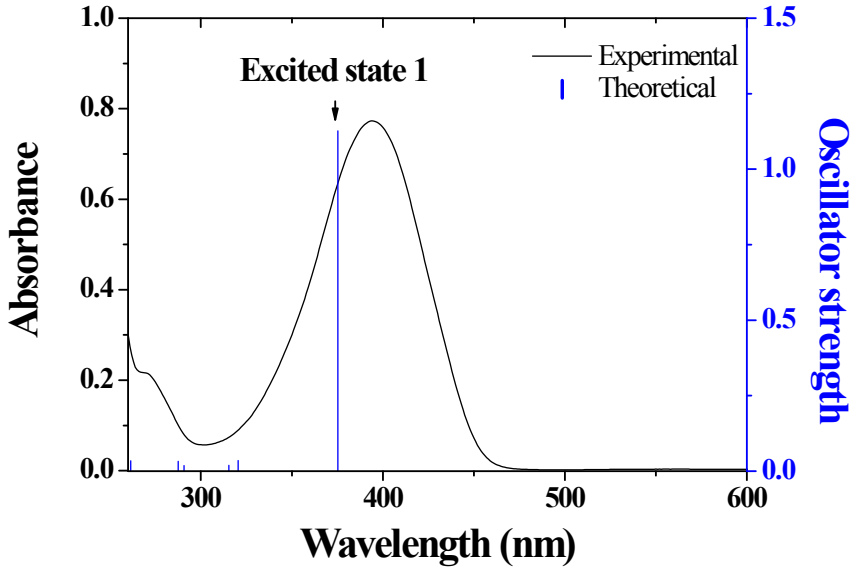

(a)

(b)

Excited State 1	Wavelength	Percent (%)	Character	Oscillator strength
H → L	375.23 nm	97	ICT	1.1265

(c)

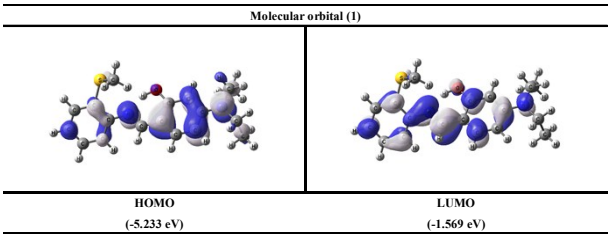

Fig. S9 (a) The theoretical excitation energies (TD-DFT method) and the experimental UV-vis spectrum of **1**. (b) The major electronic transition energy and molecular orbital contribution for **1** (H = HOMO and L = LUMO). (c) Isosurface (0.030 electron $bohr^{-3}$) of molecular orbitals participating in the major singlet excited state of **1**.

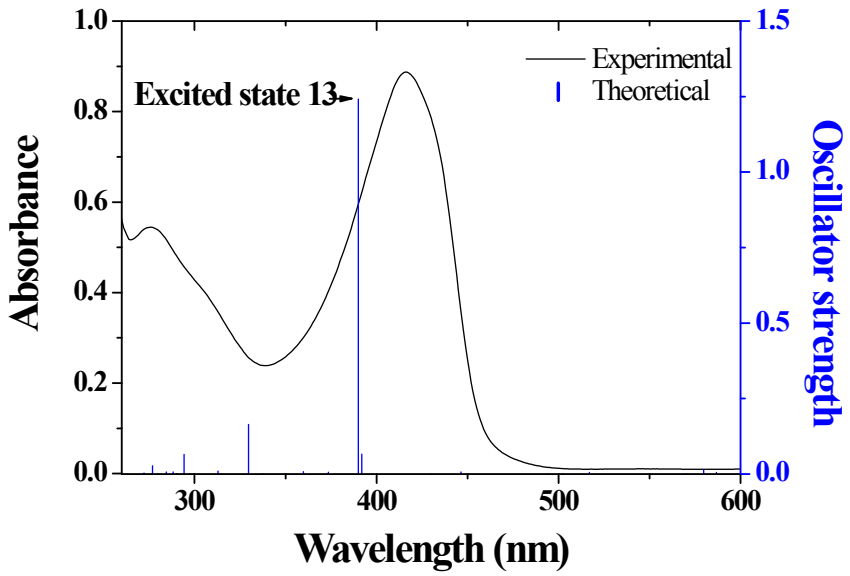

(b)

Excited State 13	Wavelength	percent (%)	Character	Oscillator strength
H (α) → L (α)	389.95 nm	40%	ICT	1.2418
H (β) → L+1 (β)		40%	ICT	
H-4 (β) → L (β)		9%	LMCT	

H-5 (β) → L (β)	3%	LMCT

(c)

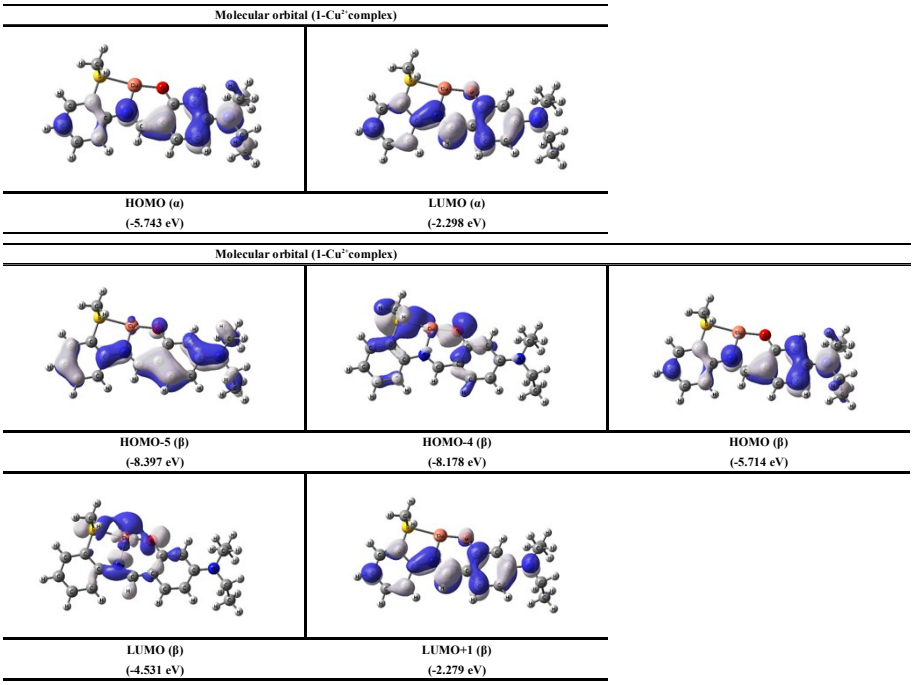

Fig. S10 (a) The theoretical excitation energies and the experimental UV-vis spectrum of **1**-Cu^{2+}. (b) The major electronic transition energies and molecular orbital contributions for

1-Cu^{2+} (H = HOMO and L = LUMO / (α): α spin MO and (β): β spin MO). (c) Isosurface (0.030 electron $bohr^{-3}$) of molecular orbitals participating in the major singlet excited states of **1**-Cu^{2+}

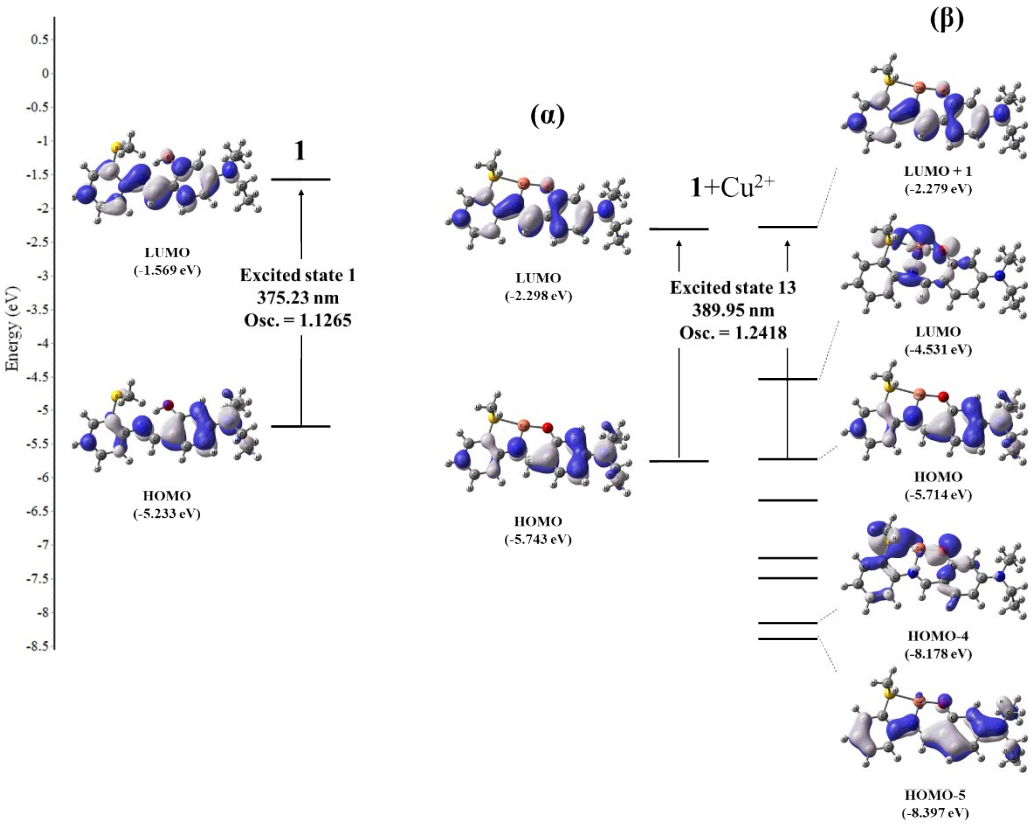

Fig. S11 Molecular orbital diagrams and excitation energies of **1** and **1**-Cu^{2+} complex.

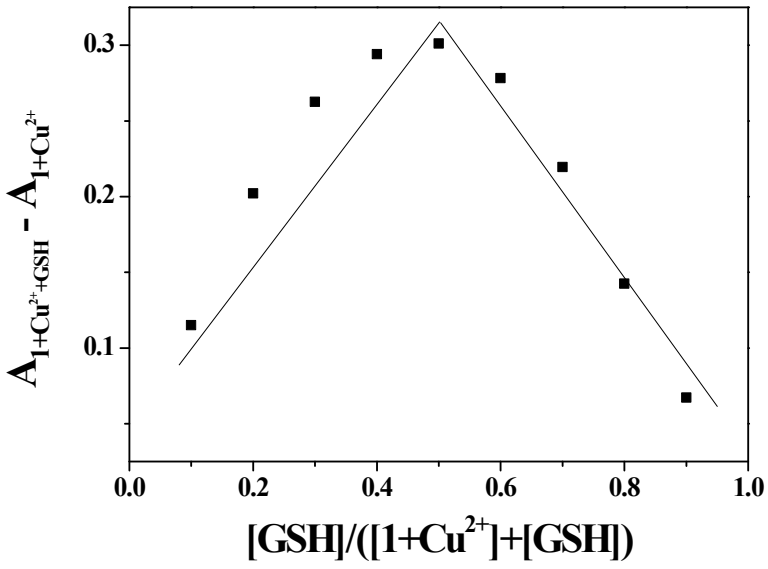

Fig. S12 Job plot of **1**-Cu^{2+} and GSH, where the intensity at 416 nm was plotted against the mole fraction of GSH. The total concentration of GSH with **1**-Cu^{2+} was 3.0×10^{-5} M.

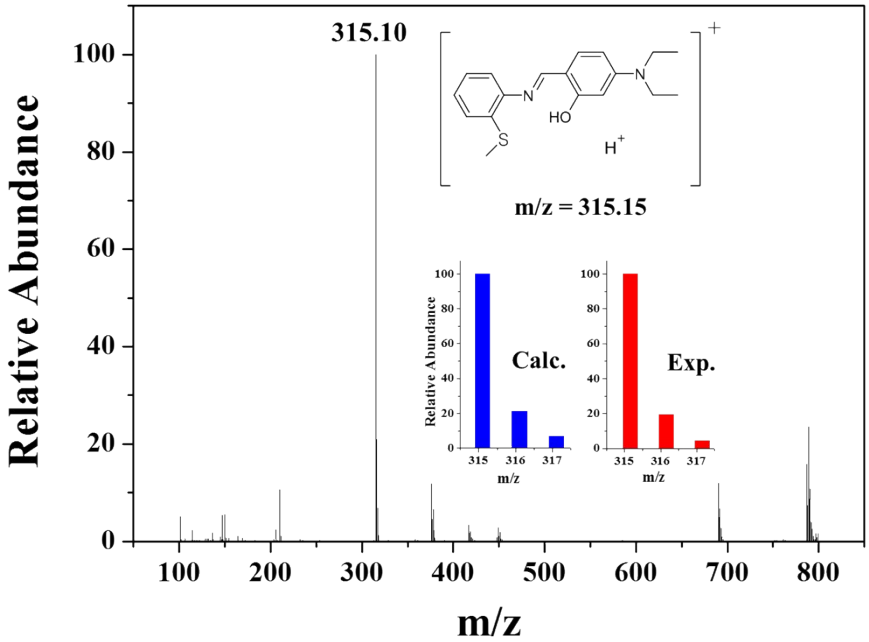

Fig. S13 Positive-ion electrospray ionization mass spectrum of **1**-Cu^{2+} (10 μM) upon

addition of 3 equiv of GSH.

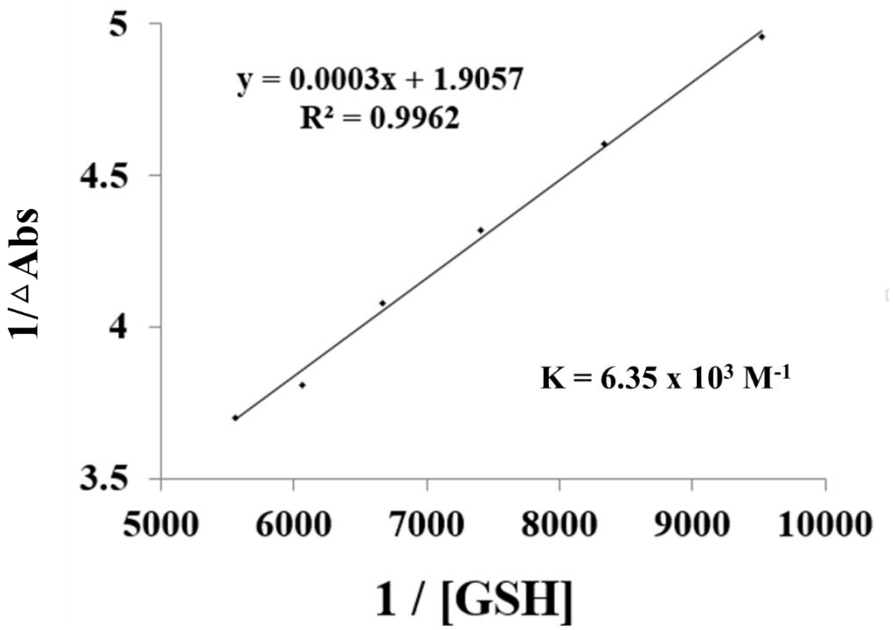

Fig. S14 Benesi-Hildebrand plot (at 416 nm) of **1**-Cu^{2+} (30 μM), assuming 1:1

stoichiometry for association between **1**-Cu^{2+} and GSH.

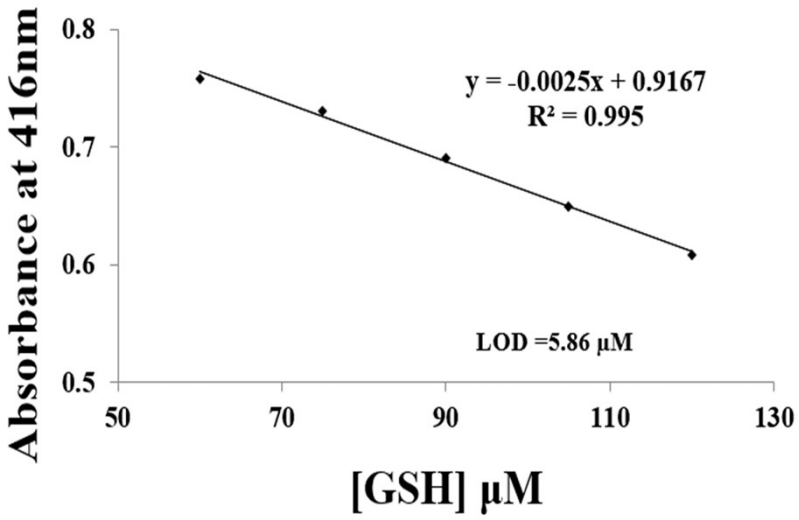

Fig. S15 Determination of the detection limit of **1**-Cu^{2+} (30 μM) for GSH based on change of absorbance at 416 nm.

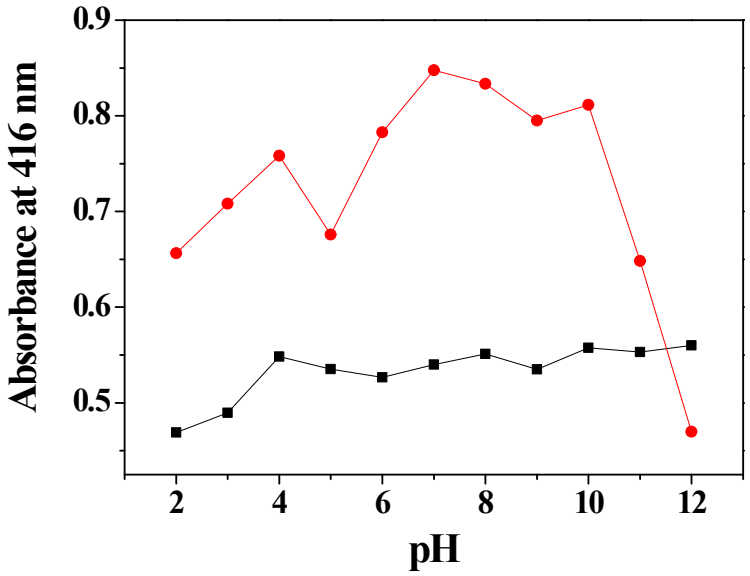
0.9
0.8
0.7
0.6
0.5
Absorbance at 416 nm
2
4
6
8
10
12
pH

Fig. S16 UV absorbance (at 416 nm) of **1**-Cu^{2+} (30 μM) and **1**-Cu^{2+}-GSH at different pH (2-12) in a mixture of DMF/bis-tris buffer (7/3, v/v), respectively.